Electronic Supplementary Material (ESI) for Nanoscale Horizons.

Supporting Information

Unravelling the switching mechanism within the coexistence of localized-interfacial switching within a single RRAM and its applications

Eng Kang Koh, [a,b] Putu Andhita Dananjaya, [a] Han Yin Poh, [a,b] Lingli Liu, [a] Calvin Xiu Xian Lee, [a,b] Jia Rui Thong,[a,b] Young Seon You,[b] and Wen Siang Lew *[a]

[a] School of Physical and Mathematical Sciences, Nanyang Technological University, 637371, Singapore.

[b] GLOBALFOUNDRIES Singapore Pte Ltd, 60 Woodlands Industrial Park D Street 2, Singapore 73806, Singapore

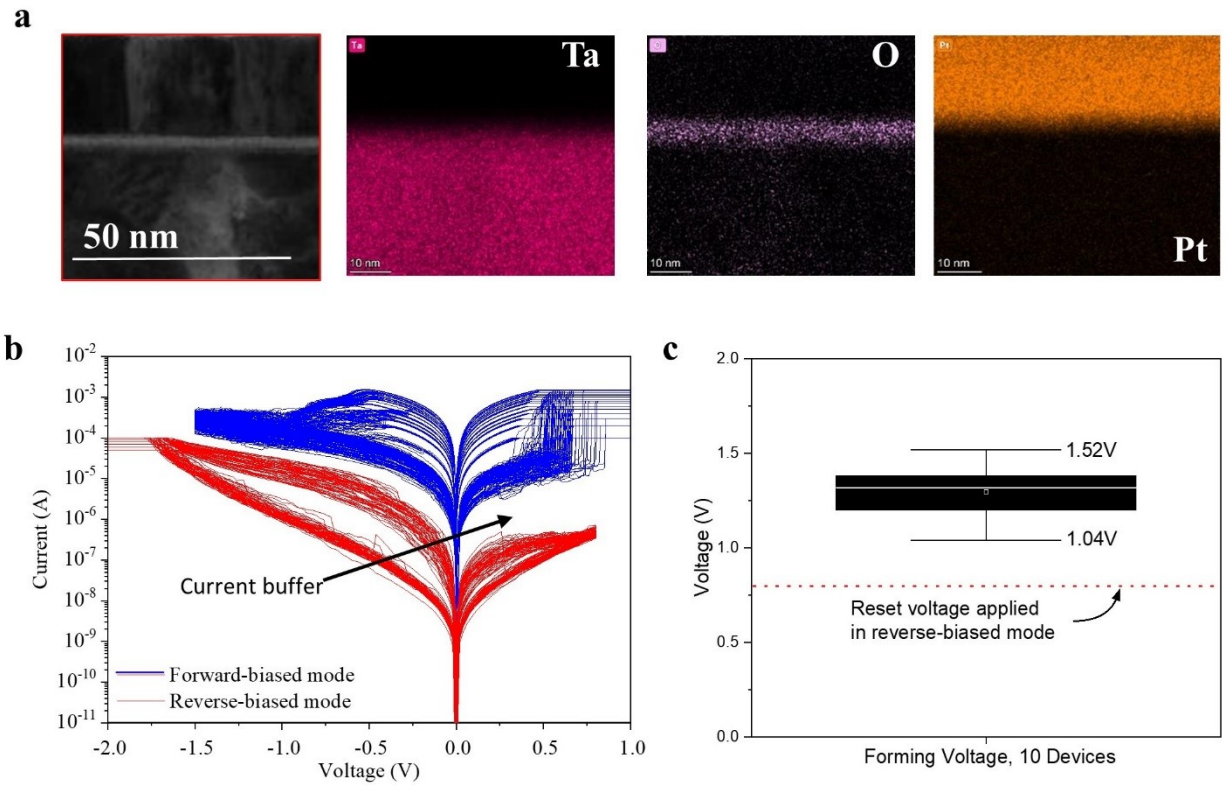

Figure S1. (a) TEM and EDS mapping for Pt, Ta, and O to verify deposited material at each layer. (b) A current buffer is present between operating the 1R device in forward and reverse-biased modes. This prevents unwanted switching of modes during practical operations. (c) Forming voltage of 10 devices. Forming operation is needed to transition the device from reverse-biased to forward-biased mode.

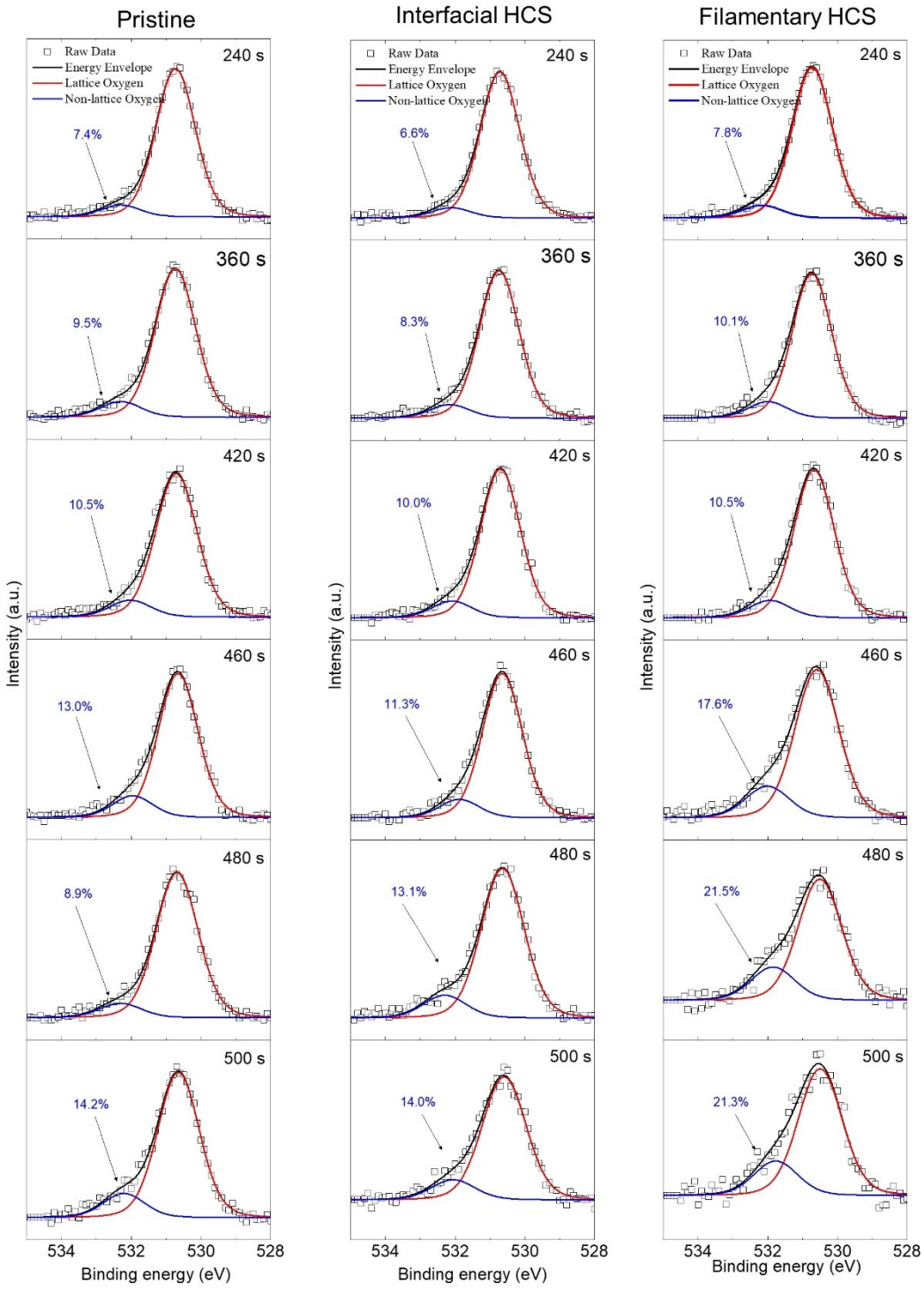

Figure S2. XPS spectra of O1s peaks of three different devices (Pristine, Interfacial HCS, and Filamentary HCS), obtained by depth profiling. Peaks have been deconvoluted into two separate peaks: Lattice and non-lattice oxygen.

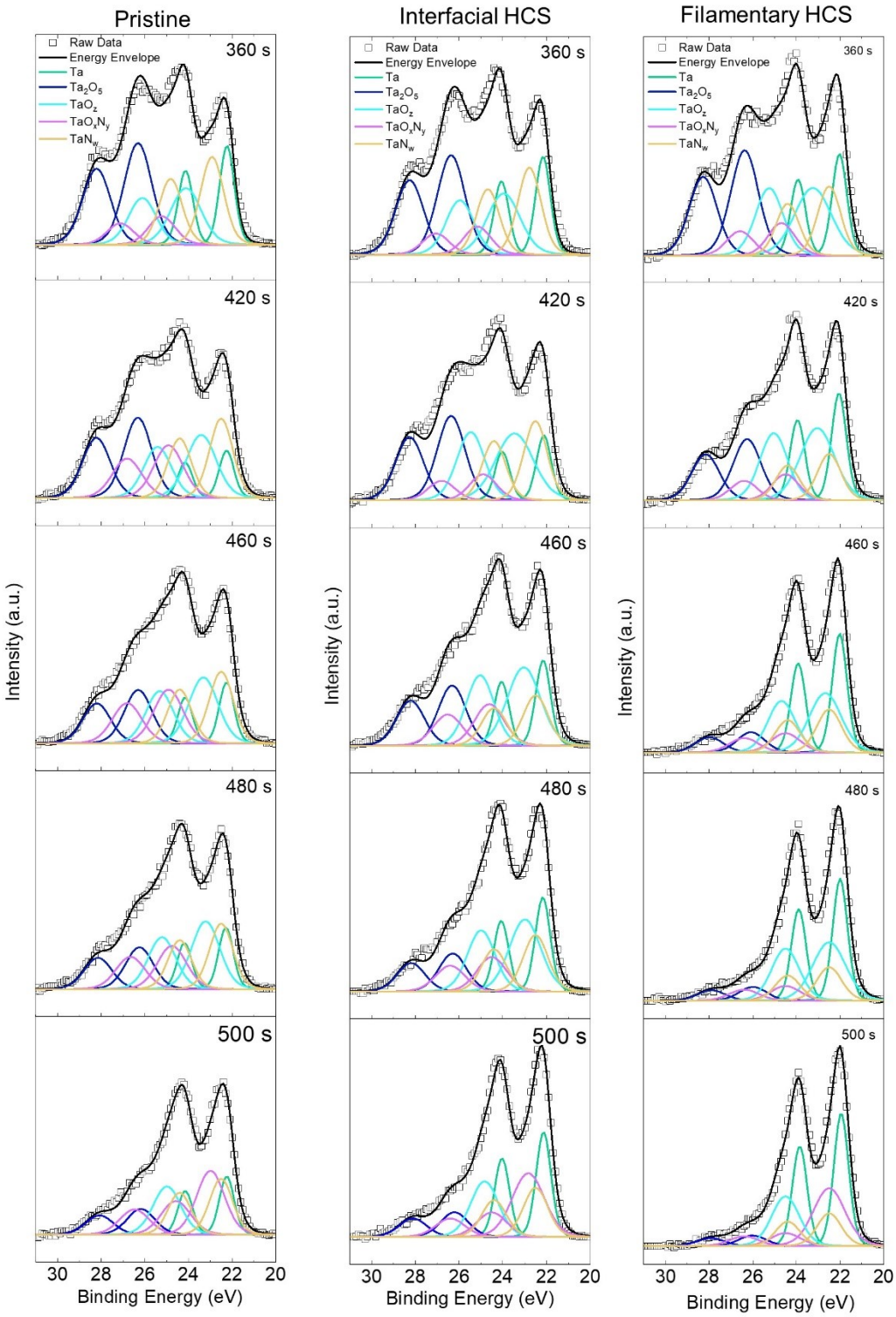

Figure S3. XPS spectra of Ta4f peaks of three different devices (Pristine, Interfacial HCS, and Filamentary HCS), obtained by depth profiling. Peaks have been deconvoluted into five separate doublets: Ta, Ta_2O_5, TaO_z, TaO_xN_y, TaN_w.

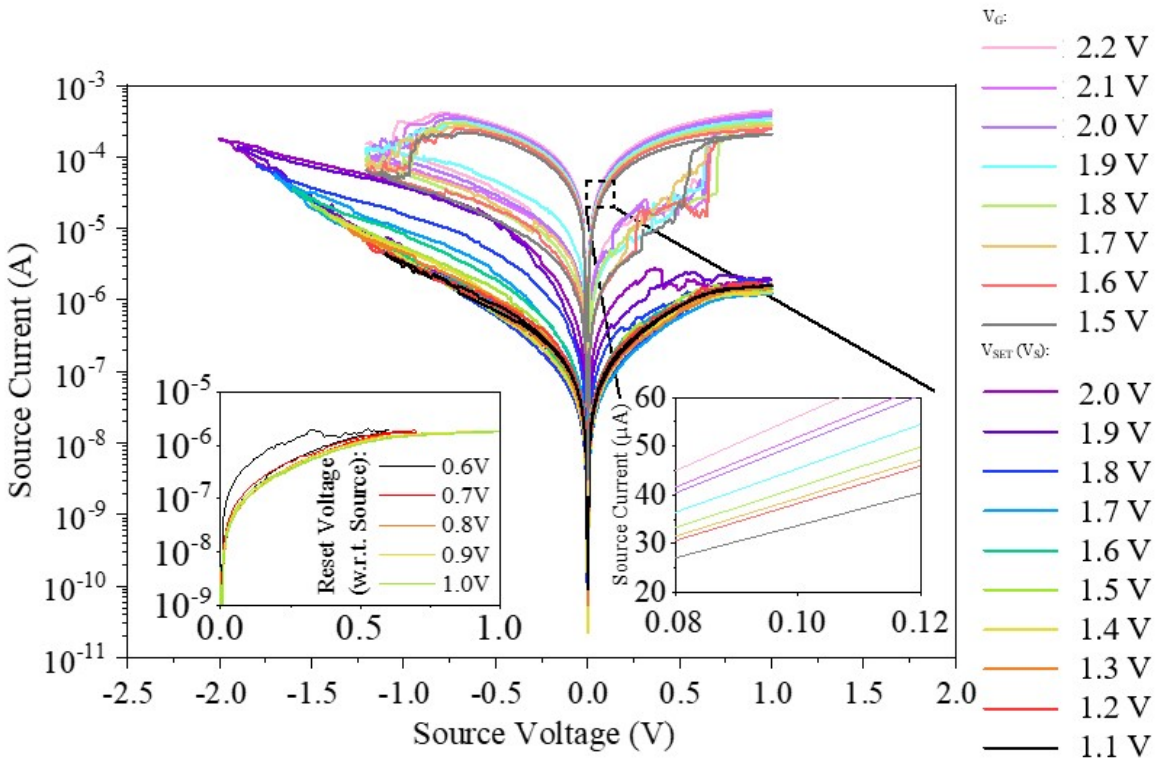

Figure S4. 1T-1R device multilevel switching demonstrated with V_G control in the forward-biased mode (1.5 V – 2.2 V). The set variation (1.1 V – 2.0 V) and reset variation (0.6 V – 1.0V, shown in the inset) were demonstrated with varying the V_S.

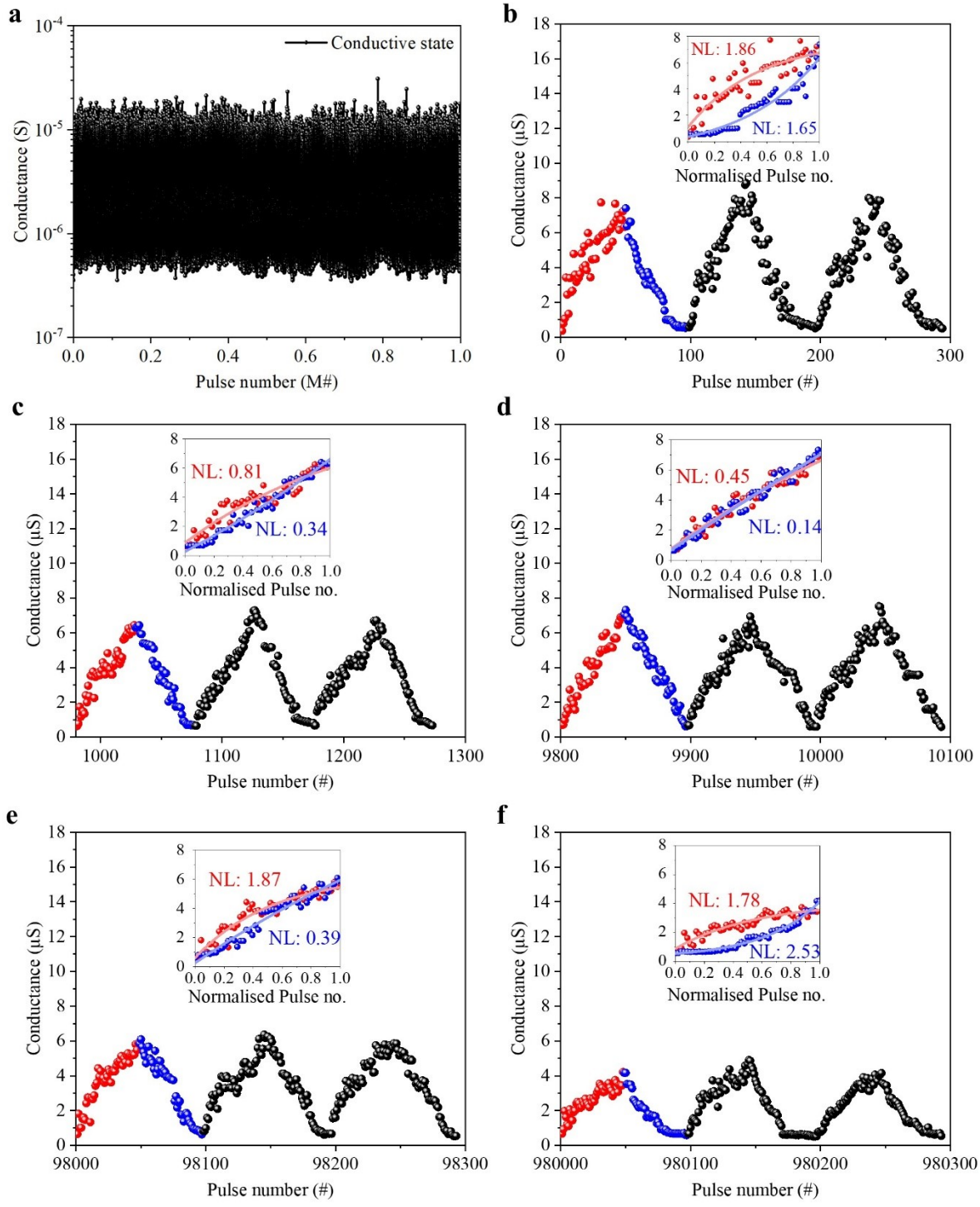

Figure S5. (a) The endurance in the reverse-biased mode operated identically to the method to obtain results shown in Figure 6a (Potentiation: -2V, 20ns – 490 ns; Depression: 2.5 V, 20ns – 490 ns); the device continued to work even after > 10^6 pulses. The PD cycles shown in Figure S4a were magnified in every order (depicted in (b), (c), (d), (e), and (f)), and the first of the three PD pulses in each figure were also fitted with NL Equations 3 and 4.

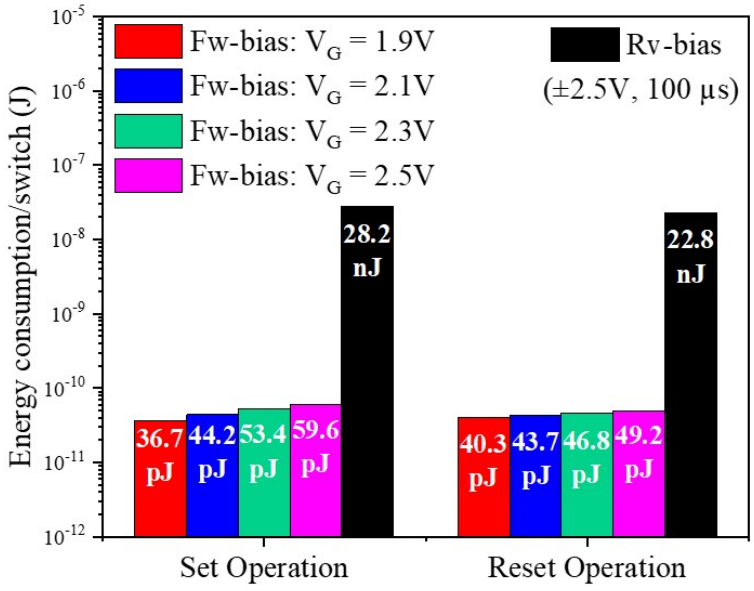

Figure S6. The energy consumption for binary switching when the device was operated in forward-biased mode was compared to if the device was operated in reverse-biased mode.

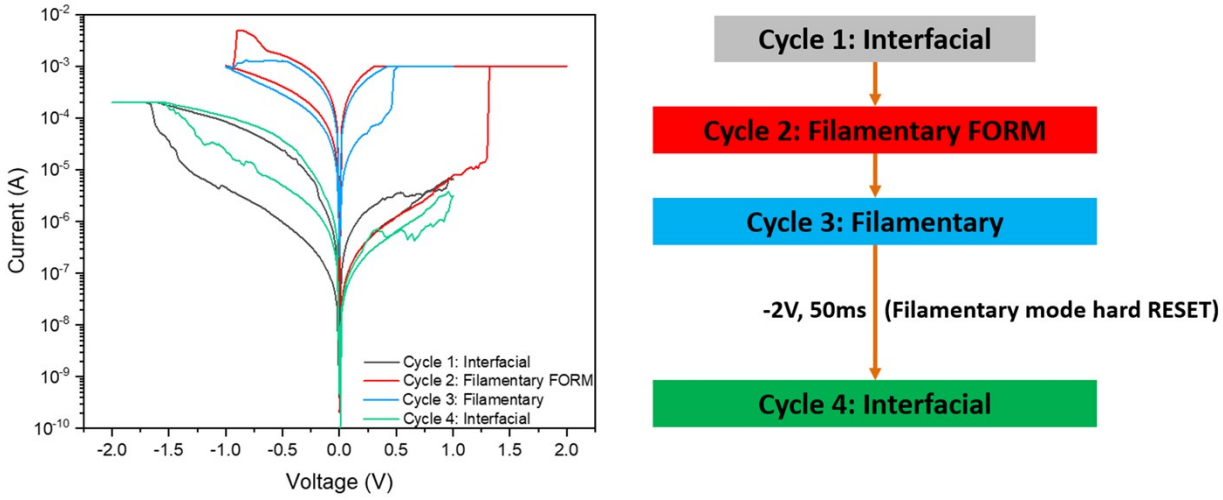

Figure S7. The device first underwent a standard set and reset process in the reverse-biased interfacial mode (grey) and subsequently a forming and first reset process in the forward-biased filamentary mode (red). This was followed by a set and reset process in the forward-biased filamentary mode (blue). The device was then subjected to a relatively long -2V pulse for ~50 ms to revert the process to the reverse-biased mode. This forced the device to undergo a hard filamentary reset, which fully retracted the filament towards the active electrode.